Computer Networks 73 (2014) 72–83

Contents lists available at ScienceDirect

Computer Networks

journal homepage: www.elsevier.com/locate/comnet

Numerical analysis of the power saving with a bursty traffic model in LTE-Advanced networks

Sunggeun Jin [a,*], Daji Qiao [b]

[a] Daegu University, Gyeongsan, Gyeongbuk 712-714, Republic of Korea
[b] Department of Electrical and Computer Engineering, Iowa State University, Ames, IA 50011, United States

ARTICLE INFO

Article history:
Received 16 February 2014
Received in revised form 14 July 2014
Accepted 3 August 2014
Available online 13 August 2014

Keywords:
3GPP LTE-Advanced
DRX
Power saving

ABSTRACT

We analyze the power saving operation called Discontinuous Reception (DRX) with a novel bursty packet arrival model in 3GPP Long Term Evolution (LTE)-Advanced networks. Typical analytical studies on the power saving operations in wireless networks have been carried out under the assumption that an expectation of exponentially distributed packet arrival intervals stays unchanged. However, practical packet arrival rate may change depending on time or typical Internet services may incur bursty packet arrivals. In either case, we need to evaluate the performance of the DRX operation. For this purpose, we develop a more realistic traffic arrival model considering packets may arrive in a bursty manner under the DRX operation. We, then, analyze the performance of the DRX operation in terms of power saving efficiency and average queuing delay, respectively. The analytical results are validated via comparisons with simulation results.

1. Introduction

Now, we are witnessing the 3GPP Long Term Evolution (LTE) wireless networks are launched to provide high speed Internet services.[1] Thanks to the 3GPP LTE networks, mobile users are allowed to enjoy high speed Internet services everywhere. In near future, the 3GPP LTE-Advanced networks are expected to be deployed for better services. So far, the wireless network issues on the power saving operations have been considered important all the time since the power saving operations are necessary to extend the lifetime of the battery-powered devices, thus improving user convenience. Accordingly, most wireless networks including IEEE 802.16/m Wireless Metropolitan Area Networks (WMANs) and IEEE 802.11 Wireless Local Area Networks (WLANs) [1–3] provide the power saving schemes. In [4–10], the authors have tried to analyze the power saving schemes for the wireless network standards. Obviously, LTE and LTE-Advanced wireless network standards specify the power saving operation called Discontinuous Reception (DRX) operation in order to reduce redundant power consumption while User Equipments (UEs) are serviced with realtime and/or lightly loaded traffic [11–14]. LTE and LTE-Advanced network technologies have evolved from the Universal Mobile Telecommunications System (UMTS). For this reason, the LTE-Advanced network's DRX operation inherits most features from the UMTS. For the purpose of analyzing UMTS' DRX operation, the authors of [15–20] made efforts to analyze the performance under the assumption that packet arrival intervals are exponentially distributed. After that, the authors of [21–23] analyzed the performance of the LTE's DRX operation with the same assumptions regarding packet arrival patterns. Recently, the authors of [24] introduced an easy way toward accurate equations for the performance analysis of the DRX operation for the

* Corresponding author. Tel.: +82 53 850 6579.
E-mail address: sgjin@daegu.ac.kr (S. Jin).

[1] In South Korea, the 3GPP LTE networks are launched in the whole country March 2012.

http://dx.doi.org/10.1016/j.comnet.2014.08.002
1389-1286/

LTE-Advanced networks. In their work, they still followed the typical assumption that packets arrive with an exponential distribution. The authors of [25] empirically measure UE's power consumption with monitoring tools in LTE systems. Their measurements are used to estimate UE's state transitions under affirmative assumption that sudden surge of power consumption might indicate packet transmissions and receptions. However, the measurements are conducted in not eNode-B but UE so that they are limited in representing realistic packet arrivals in eNode-B. In [26], VoIP traffic is focused without any specific analytical modeling.

Typical Internet services such as web surfing and messengers tend to generate sporadic traffic, and hence it would be realistic to consider bursty packet arrivals for the services [27,28]. From this consideration, the authors of [29] first analyzed the performance of the power saving operation for the UMTS networks with bursty packet arrival model provided by ETSI [30]. For our explanation, we call the previously studied model *ETSI model*.

Now, we briefly review the *ETSI model* and the numerical analysis introduced in [29] as follows: (1) a session consists of multiple packet calls. (2) Likewise, each packet call has multiple packets. (3) In the ETSI model, the packet arrival intervals are assumed to be too short for an UE to enter the DRX. Accordingly, the UE should keep awake between consecutive packet arrival instants. (4) The number of calls/packets in a session/call is assumed to be geometrically distributed. (5) The idle time between an instant of a session completion and a beginning instant of its subsequent session is assumed to follow exponential distribution. It implicates that new session/call arrivals are not allowed when current session/call is serviced. (6) The call service times follow a Pareto distribution.

However, there are some drawbacks of the ETSI model. (1) In the model, it is assumed that a new session does not begin until the completion of current session. Practically, this assumption may be unrealistic since a new session/call may arrive while current session/call is serviced. Actually, against their assumption, it is more reasonable to assume that a new session/call may begin/arrive while current session/call is serviced. (2) It is more comprehensive to assume the call service times follow a general distribution rather than a particular distribution, e.g., Pareto distribution. (3) The ETSI model is unnecessarily complicated. As already explained, packets are grouped into a call, and then, calls generates a session. However, in the ETSI model, the UE keeps awake during packet interarrival times so that a call is actually treated as a transmission unit. In contrast to the ETSI model, it is better to consider that a call is equivalent to a long single packet having multiple small-sized packets. In this case, we can deal with the long single packet for a transmission. For this reason, in the rest of this paper, we adopt the term of packet rather than the term of call. As detailed later, we consider that a new call may arrive during ongoing call service times. In the proposed model, call service times follow general a distribution. Therefore, the proposed model can cover the ETSI model. Nevertheless, the proposed model is simpler than the ETSI model.

The paper is organized as follows: in Section 2, we elaborate on our bursty packet arrival model for the numerical analysis. In Section 3, we explain the DRX operation in the 3GPP LTE-Advanced networks. In Section 4, we provide numerical analysis for the power saving efficiency and the average queuing delay, respectively. In Section 5, we validate the numerical equation derivations via comparisons with simulation results. Finally, Section 6 concludes this paper.

2. Bursty packet arrival model

We provide a novel traffic arrival model. In our model, a series of bursty packets arrive with short intervals. However, at the end of the bursty packet arrivals, packet arrival intervals become longer than the bursty packet arrival intervals. Additionally, the packets may arrive during ongoing packet transmission times. Our model is clearly different from what ETSI proposed and discussed in [29,30]. Then, we summarize the differences as follows: (1) we consider the case when new packets may arrive while eNode-B is forwarding its buffered packets toward the UE in the DRX operation. In contrast, there is no way to handle this case in the ETSI model. (2) When a packet is transmitted, it may experience various types of wireless channels, e.g., Rician, Additive White Gaussian Noise, and Rayleigh channels. Therefore, it is needed to consider general cases for wireless channel quality. For this reason, we consider packet transmission times are generally distributed while the packet transmission times follow Pareto distribution in the ETSI model. (3) We consider that a packet may arrive during ongoing packet transmission time while a new packet arrives after the transmission completion of previously arriving packet in the ETSI model. (4) Our model has additional feature that packet arrival rate may change as time elapses.

Fig. 1 illustrates an example for the proposed bursty packet arrival model. In this model, we can observe a series of consecutive packet arrivals spaced with short intervals in a bursty manner. During the period for the bursty packet arrivals, a subsequent packet may arrive with the packet arrival probability (=p) of a geometric distribution. Note that new packets may arrive during ongoing packet transmission time. Those packets are temporarily buffered, and thereafter consecutively forwarded to the DRX UE. Therefore, the bursty packet arrivals are terminated with the probability of $1-p$. In this period, the packet arrivals are exponentially distributed with the expectation of $1/\lambda_B$. λ_B is an average packet arrival rate for busy packets. It implies that a new period, in which packet arrivals are sparsely scattered, begins with the probability of $1-p$. When the new period begins, subsequent packets arrive with the probability of q of a geometric distribution. λ_I indicates the packet arrival rate for this case. The packet arrival intervals follows an exponential distribution. New bursty packet arrivals may follow sparse packet arrivals with probability of $1-q$. Meanwhile, we assume that packet transmission times follow a general distribution irrespective of bursty packet arrivals or not.

Our packet arrival model can cover typical bursty packet arrival models in which bursty packet arrivals appear intermittently when $q=0$ and $1/\lambda_B \ll 1/\lambda_I$. In this

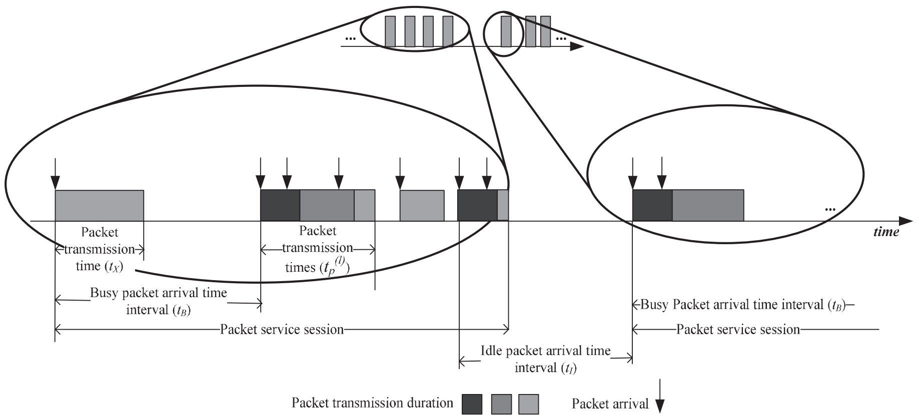

Fig. 1. An exemplary bursty packet arrivals.

case, a series of consecutive packets arrive with short time intervals intensively for a while, and then such intensive packet arrivals stop. However, a new series of packet arrivals begins after the expected period of $1/\lambda_I$. On the other hand, the proposed packet arrival model is also useful for handling the changes of packet arrival rates depending on time when $q \neq 0$. In the proposed model, it can be considered that packet arrival rate changes after the end of bursty packet arrivals. In summary, the packet arrival rate varies from the expectation of $1/\lambda_B$ to the expectation of $1/\lambda_I$. We can manage the packet arrival rate changes by adjusting p and q.

From the proposed packet arrival model, we analyze the performance of the DRX operation in the 3GPP LTE-Advanced networks. For our explanation, we adopt the terms of *busy* and *idle* connoting bursty packet arrivals and sparse packet arrivals. In other words, busy packet arrivals implicate that packets arrive with short intervals of expectation $1/\lambda_B$. Similarly, idle packet arrivals imply that packets arrive with long arrival intervals with the expectation of $1/\lambda_I$. It is because session arrivals with a single packet are identical to packet arrivals of which intervals are exponentially distributed with expectation $1/\lambda_I$. Prior to the analysis, we first explain the DRX operation. It is designed to save power consumption for UEs (UE) in the 3GPP LTE-Advanced wireless networks.

3. DRX operation in 3GPP LTE-Advanced wireless networks

Fig. 2 illustrates an exemplary operation for the case when a UE conducts the DRX operation. The UE periodically wakes up to monitor new packet arrivals in a period of a DRX cycle. At the beginning of a DRX cycle, the UE temporarily stays awake to receive an indication message. If the UE receives a negative indication message, the UE inactivates its transceiver for sleeping. Otherwise, the UE stays awake to receive eNode-B's buffered packets. Indication message transmission time is negligibly short, and hence we ignore the indication message transmission time for our analysis. In this figure, DRX cycles are indicated by rectangles with letters 'S' and 'L' standing for short and long DRX cycles, respectively.

According to [24], there are four operational states for proper analysis. First, we define *activity period* by the time duration from time instant that the eNode-B begins to transmit packets to the time instant that eNode-B's buffer becomes empty due to the completion of packet transmissions. Second, *first activity period* is defined by the activity period following DRX cycles. Third, we define *inactivity period* by the time duration when an inactivity timer is activated as specified by the 3GPP LTE-Advanced standard [11]. Lastly, *active state* is defined for the time duration from the beginning of the first activity period to the time instant of inactivity timer's expiration.

We explain how the UE manages the DRX operation in detail. When eNode-B's buffer becomes empty after completing buffered packet transmissions, the UE activates an inactivity timer prior to sleeping with DRX cycles. Unless at least one packet arrive within the timer's timeout, the UE begins to sleep. If there are new packet arrivals prior to the timer's expiration, the UE has another activity period to receive those packets. Then, the activity period may keep prolonged as long as more packets arrive at the eNode-B during ongoing packet transmission times. In other words, activity periods are repeatedly interleaved with inactivity periods until the inactivity timer expires.

Sleeping state begins with inactivity timer's expiration. In sleeping state, the UE monitors new packet arrivals at the eNode-B by receiving indication messages every DRX cycle. The DRX cycles follow back-to-back until new packet arrivals. If the UE detects new packet arrivals, operational state transits to active state for the UE to receive those packets during activity period. Optionally, short DRX cycle can be employed for more frequent packet arrivals than long DRX cycle's. There may exist services with aperiodic silent period or occasional packet arrivals. In this case, long DRX cycle may be useful. Long DRX cycles begin after the maximum number (=N) of short DRX cycles has passed without new packet arrivals. N is configurable value. Prior to the numerical analysis in the subsequent section, we summarize all notations for it shown in Table 1.

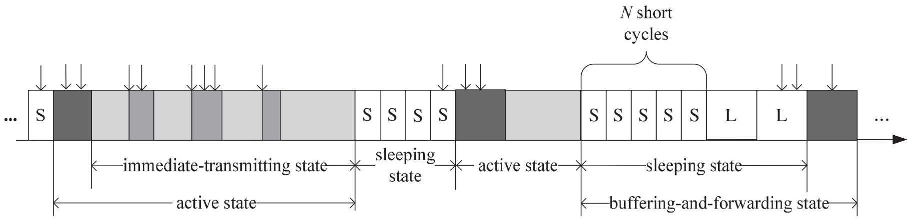

Fig. 2. An example of the DRX operation in 3GPP LTE-Advanced wireless networks.

Table 1
Notations.

Notation	Meaning	Notation	Meaning
λ	Overall packet arrival rate	λ_A	Packet arrival rate in active state
λ_B	Busy packet arrival rate	λ_I	Idle packet arrival rate
φ_i	Probability for the inactivity timer expires after the *i*th timer (re) starting	–	–
π_B	Stationary probability for state S_B	π_I	Stationary probability for state S_I
ρ	Overall offered load	ρ_A	Offered load for active packet arrivals
τ	Packet transmission time	ψ_j	Probability for a new packet arrival at *j*th short or long DRX cycle after inactivity timer expiration
C_L	Time duration for long DRX cycle	C_S	Time duration for short DRX cycle
C_T	Time duration for inactivity timer	N	Maximum number for short DRX cycles before the beginning of long DRX cycles
S_B	State for busy packet arrivals	S_I	State for idle packet arrivals
T_A	Expected time for UE's active state	T_D	Expected time for UE's inactive state
p	Busy packet arrival probability in state S_B	q	Idle packet arrival probability in state S_I
p_B	Probability for the busy packet arrival interval short enough to prevent the UE from beginning DRX operation	p_I	Probability for the idle packet arrival interval short enough to prevent the UE from beginning DRX operation
$\overline{p}_B$	Probability for the busy packet arrival interval long enough to begin the DRX operation	$\overline{p}_I$	Probability for the idle packet arrival interval long enough to begin the DRX operation
t_B	Busy packet arrival time interval	t_I	Idle packet arrival time interval
t_X	Packet transmission time	t_p	The packet transmission times required for a packet and its subsequently arriving packets during ongoing packet transmission times
$\tilde{t}_p$	The expected first activity period	$\hat{t}$	The expectation of the inactivity timer duration for the busy and idle packets in steady state
t_L	The sleeping times provided by long DRX cycles	t_S	The sleeping times provided by short DRX cycles
$\hat{t}_B$	The expectation of the inactivity timer duration for the busy packets	$\hat{t}_I$	The expectation of the inactivity timer duration for the idle packets

4. Analysis

4.1. Preliminary

Fig. 3 illustrates an *embedded Markov process* reflecting the rate changes of the arriving packets. State S_B (or S_I) indicates that busy (or idle) packets arrive with probability of p (or q). In state S_B (or S_I), packet arrival intervals are exponentially distributed with the expectation of $1/\lambda_B$ (or $1/\lambda_I$). From the Markov process, we can summarize that the packets in state S_B arrive in a bursty manner while the packets in state S_I arrive intermittently. State S_B (or S_I) may transit to state S_I (or S_B) with probability $1-p$ (or $1-q$). For proper analysis, let π_B and π_I indicate the stationary probabilities for states S_B and S_I, respectively in steady state. From this figure, we have the stationary probabilities π_B and π_I by:

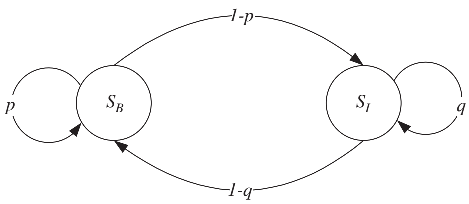

Fig. 3. An embedded Markov chain reflecting the changes of the packet arrivals.

$$\pi_B = \frac{1-q}{2-(p+q)}, \tag{1}$$

$$\pi_I = \frac{1-p}{2-(p+q)}. \tag{2}$$

We also need to derive the packet arrival rate in the case when two types of packet arrivals are mixed. For this purpose, we define the *equivalent packet arrival rate* assuming two types of packet arrival intervals are averaged over infinite time. In the steady state, the expected packet arrival interval of the equivalent packet arrival rate is equal to weighted sum of the two types of packet arrival intervals. In this sense, the equivalent packet arrival rate is derived by:

$$\lambda = \lim_{T\to\infty}\left(\frac{1}{\pi_B\frac{1}{\sum_{j=0}^{\infty}\frac{\lambda_B T}{j!}e^{-\lambda_B T}}+\pi_I\frac{1}{\sum_{j=0}^{\infty}\frac{\lambda_I T}{j!}e^{-\lambda_I T}}}\right)\Big/ T$$
$$= \frac{\lambda_I\lambda_B}{\pi_B\lambda_I+\pi_I\lambda_B}. \tag{3}$$

For further derivations, it is necessary to derive the equation for the time required to complete packet transmissions. In fact, more new packets may arrive during ongoing packet transmission time. In this case, the arriving packets during ongoing packet transmission time are temporarily buffered in the eNodeB until the completion of the ongoing packet transmission. Then, the buffered packets are forwarded to the UE at the end of packet transmission one by one until the buffer becomes empty. It implies that UE's listening window may extend for the continuous packet receptions. Fig. 4 illustrates how a single packet transmission contributes to the listening window extensions while more packets arrive during ongoing packet transmissions. In this figure, random variable t_X represents the time required to transmit a single packet. On the other hand, random variable $t_p^{(l)}$ indicates the overall packet transmission time from starting instant of a packet transmission to ending instant of continuing subsequent packet transmissions due to the case when no more packets arrive during ongoing packet transmissions. It can be recursively defined as follows:

$$t_p^{(l)} = t_X + \sum_{m\in\mathcal{M}} t_p^{(m)}, \tag{4}$$

where $\mathcal{M}$ is set of arriving packets during ongoing transmission of packet m. $t_p^{(m)}$'s are mutually independent random variables with the same distribution. Then, we can have the Laplace transform of this equation by:

$$E\left[e^{-st_p^{(l)}}|t_X=t\right] = e^{-st}\left(F^*_{t_p}(s)\right)^{|\mathcal{M}|}, \tag{5}$$

where $F^*_{t_p}(s)$ is the Laplace transform of t_p. In this case, it is satisfied that subsequently arriving packets prevent the UE from entering DRX operation. Note that the packet arrival rate is different from the equivalent packet arrival rate

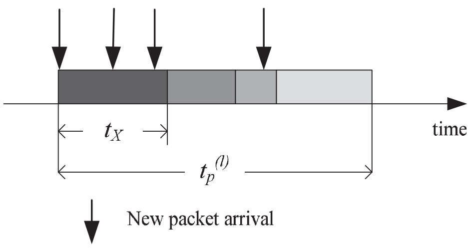

Fig. 4. An example for the times required for a packet and its subsequently arriving packets during ongoing packet transmission times.

under this condition. Therefore, we need to derive the packet arrival rate for the condition. For convenience, we call the packet arrival rate for the condition as *active packet arrival rate* denoted with λ_A.

We adopt two random variables, i.e., t_B and t_I, representing busy and idle packet arrival intervals, respectively. Due to the memoryless property of the exponential distribution, it is satisfied that $\Pr(t_B > t_X + C_T | t_B \geqslant t_X) = \Pr(t_B > C_T)$ for random variable t_B. Then, we can derive the probability $\Pr(t_B > C_T)$ that new arriving packet makes the UE begin the DRX operation by $\Pr(t_B > C_T) = \int_{C_T}^{\infty} e^{-\lambda_B t}dt = e^{-\lambda_B C_T}$. The same is true of random variable t_I. Herein, we derive the probability that the packet arrival interval is short enough to prevent the UE from beginning DRX operation for either busy or idle packet arrival interval by:

$$p_B = (1-e^{-\lambda_B C_T})\pi_B, \tag{6}$$
$$p_I = (1-e^{-\lambda_I C_T})\pi_I. \tag{7}$$

Similarly, we can also derive the probability that the packet arrival interval is sufficiently long so that the UE enters the DRX operation by:

$$\overline{p}_B = e^{-\lambda_B C_T}\pi_B, \tag{8}$$
$$\overline{p}_I = e^{-\lambda_I C_T}\pi_I. \tag{9}$$

From Eq. (6), we have the active packet arrival rate ($=\lambda_A$) by:

$$\lambda_A = 1\Big/\left(\frac{1}{\lambda_B}\frac{p_B}{p_B+p_I}+\frac{1}{\lambda_I}\frac{p_I}{p_B+p_I}\right). \tag{10}$$

Then, we have the time required to complete consecutive packet transmissions incurred by a new packet arrival at empty eNode-B's buffer by:

$$\begin{aligned}F^*_{t_p}(s) &= E\left[e^{-st_p^{(l)}}\right]\\ &= \int_0^{\infty}\sum_{j=0}^{\infty} e^{-st}F^*_{t_p}(s)^j\frac{(\lambda_A t)^j}{j!}e^{-\lambda_A t}dF_{t_X}(t)\\ &= \int_0^{\infty}\exp\left(-t(s+\lambda_A-\lambda_A F^*_{t_p}(s)\right)dF_{t_X}(t)\\ &= F^*_{t_X}\left(s+\lambda_A-\lambda_A F^*_{t_p}(s)\right),\end{aligned} \tag{11}$$

where $F_{t_X}(t)$ and $F^*_{t_X}(s)$ are cumulative density function (cdf) and the Laplace transform of random variable t_X, respectively. Furthermore, since $E[t_X] = -dF^*_{t_X}(s)/ds|_{s=0} = \tau$ and $F^*_{t_X}(0) = F^*_{t_p}(0) = 1$, we have:

$$E[t_p] = -dF^*_{t_p}(s)/ds|_{s=0} = \frac{\tau}{(1-\rho_A)}, \tag{12}$$

where $\rho_A = \lambda_A\tau$. ρ_A is defined as offered load for active packet arrivals.

4.2. Power saving factor

The *power saving factor* is typically used to represent power saving efficiency that how long the DRX UE sleeps compared with overall operating time. It is a ratio between average sleeping time and the overall operating time so that it is obtained by dividing the average sleeping time by the entire DRX operation time. It is given by [24]:

$$\frac{E[T_D]}{E[T_A]+E[T_D]}, \tag{13}$$

where $E[T_D]$ and $E[T_A]$ represent the expected times when the UE is in inactive and active states, respectively. Note that the overall time when the UE is in inactive state is equal to the overall sleeping time. For this equation, we derive the time periods where the UE stays in inactive and active states, respectively. Accordingly, we need to have the equations about how many DRX cycles the UE should experience until terminating the DRX operation. Recalling the memoryless property of the exponential distribution, it is satisfied that $\Pr(t_B > C_S + t_X + C_T | t_B \geqslant t_X + C_T) = \Pr(t_B > C_S)$. From this property, we can derive the probability that busy or idle packet arrival interval is longer than a short DRX cycle by:

$$\Pr(t_B > C_S) = \int_{C_S}^{\infty} e^{-\lambda_B t}\,dt = e^{-\lambda_B C_S}. \tag{14}$$

$$\Pr(t_I > C_S) = \int_{C_S}^{\infty} e^{-\lambda_I t}\,dt = e^{-\lambda_I C_S}. \tag{15}$$

By using these equations, we derive the probability ψ_j that a new packet arrives at jth short or long DRX cycle after inactivity timer expiration. Thanks to the memoryless property again, it is possible to have the probability $\Pr(t_B > jC_S)$ with a product of $\Pr(t_B > C_S)$'s. As explained earlier, the UE may sleep until a new packet arrives once it enters the DRX operation. Unless a new packet arrives during first N short DRX cycles, the UE begins to sleep in units of long DRX cycle. Therefore, we derive the probability ψ_j considering two cases when $1 \leqslant j \leqslant N$ and $N < j$, respectively. First, for the case when $1 \leqslant j \leqslant N$, the probability ψ_j is derived by:

$$\begin{aligned}\psi_j &= \Pr(jC_S < t_B \leqslant (j+1)C_S) + \Pr(jC_S < t_I \leqslant (j+1)C_S)\\ &= \overline{P}_B (e^{-\lambda_B C_S})^{j-1}(1-e^{-\lambda_B C_S}) + \overline{P}_I (e^{-\lambda_I C_S})^{j-1}(1-e^{-\lambda_I C_S}).\end{aligned} \tag{16}$$

where $\overline{P}_B = \overline{p}_B/(\overline{p}_B+\overline{p}_I)$ and $\overline{P}_I = \overline{p}_I/(\overline{p}_B+\overline{p}_I)$. Next, for the case when $N < j$, we can derive the probability ψ_j by:

$$\begin{aligned}\psi_j &= \overline{P}_B\Big((e^{-\lambda_B C_S})^N (e^{-\lambda_B C_L})^{j-(N+1)}(1-e^{-\lambda_B C_L})\Big)\\ &\quad + \overline{P}_I\Big((e^{-\lambda_I C_S})^N (e^{-\lambda_I C_L})^{j-(N+1)}(1-e^{-\lambda_I C_L})\Big),\end{aligned} \tag{17}$$

where C_L and C_S indicate the durations for long and short DRX cycles, respectively. Assuming random variables t_S and t_L indicate the sleeping times provided by short and long DRX cycles, respectively. Additionally, $E[t_S]$ and $E[t_L]$ are their expectations. The reason why we consider $E[t_S]$ and $E[t_L]$ is that the overall sleeping time $E[T_D]$ consists of short and long DRX cycles. From Eq. (8), we can derive $E[T_D]$ by:

$$\begin{aligned}E[T_D] &= E[t_S] + E[t_L] = \sum_{j=1}^{N} j\psi_j C_S + \sum_{j=N+1}^{\infty}(j-N)\psi_j C_L\\ &= \left(\overline{P}_B\left(\frac{1-(e^{-\lambda_B C_S})^N}{1-e^{-\lambda_B C_S}}\right) + \overline{P}_I\left(\frac{1-(e^{-\lambda_I C_S})^N}{1-e^{-\lambda_I C_S}}\right)\right)C_S\\ &\quad + \left(\overline{P}_B\left(\frac{(e^{-\lambda_B C_S})^N}{1-e^{-\lambda_B C_L}}\right) + \overline{P}_I\left(\frac{(e^{-\lambda_I C_S})^N}{1-e^{-\lambda_I C_L}}\right)\right)C_L.\end{aligned} \tag{18}$$

We continue to derive the expected awake time $E[T_A]$. The awake time consists of the times required for packet transmissions and inactivity timer's operation. In fact, we already have the equation for time required to transmit a packet arriving at empty eNode-B's buffer and its subsequent packets arriving during ongoing packet transmission times. From Eq. (4), we extend the equation for the time, called the first activity period, representing how long time is needed to transmit the packets arriving during not only the DRX operation but also ongoing packet transmission times. The first activity period begins with the packets buffered during the DRX cycles prior to the first activity period, and hence it can be observed that $\lambda E[T_D]$ packets stay buffered at the beginning of the first activity period. From this observation, we derive the expected first activity period denoted by $E[\tilde{t}_p]$ as follows:

$$E[\tilde{t}_p] = \lambda E[T_D]\frac{\tau}{1-\rho_A} = E[T_D]\frac{\rho}{1-\rho_A}, \tag{19}$$

where $\rho = \lambda\tau$. Then, we derive the time for inactivity timer's operation.

Fig. 5 illustrates the operation of the inactivity timer. In this figure, a packet may arrive between the instant that packet transmissions are completed and the instant that inactivity timer expires. In this case, the arriving packet is immediately forwarded to the UE. However, eNode-B buffers the arriving packets after the inactivity timer expiration. Herein, we derive the probability φ_i that the

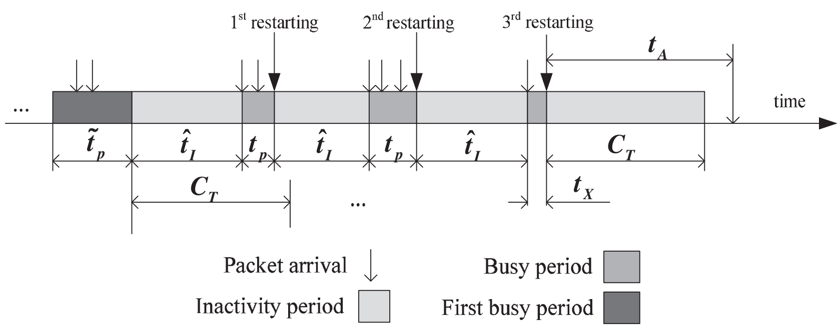

Fig. 5. Time durations when the UE is in active state.

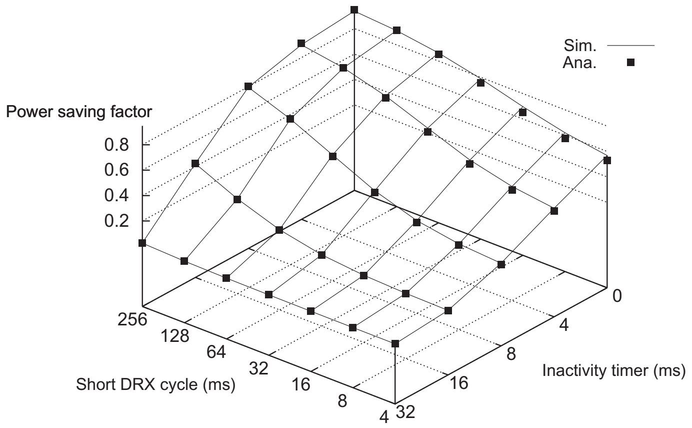

(a) Power saving factor.

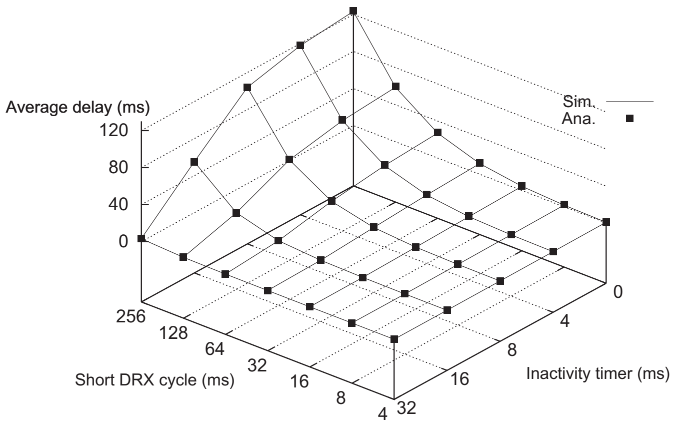

(b) Average queuing delay.

Fig. 6. Power saving factor and average queuing delay when $R = 0.1,\ N = 4,\ p = 0.8,\ q = 0.2,\ \tau = 0.1,\ \lambda_B = 1$ and $C_L = 2C_S$.

inactivity timer expires after the ith (re) starting since we need the extended awake time due to the inactivity timer's operations. We derive the probability φ that new packet arrives prior to inactivity timer expiration by:

$$\varphi = \overline{p}_B + \overline{p}_I. \tag{20}$$

The active state time period increases repeatedly as long as new packets arrive during the period of ongoing inactivity timer. It implies that we can have the probability that inactivity timer restarts ith times by $(\varphi)^i$. Meanwhile, the inactivity timer expires with probability of $1 - \varphi$. Therefore, we can derive the probability φ_i that the inactivity timer expires after ith (re) starting as follows:

$$\varphi_i = (\varphi)^i (1 - \varphi). \tag{21}$$

By using this equation, we continue to derive the awake time extended by inactivity timer's restartings. In order for the inactivity timer to stop, a new packet should arrive before the timer's expiration. However, the packet arrival rate may be different depending on the stationary states S_B and S_I. Actually, we can adopt $\overline{p}_B$ and $\overline{p}_B$ representing the stationary probabilities for states S_B and S_I under this condition.

Since there are two types of arriving packets are mixed, we need to consider the two types of inactivity timer durations between the instant when inactivity timer restarts and the instant when a new packet arrives within the inactivity timer's timeout. When $C_T > 0$, we first the expectation of the inactivity timer duration for the busy packets by:

$$E[\hat{t}_B] = \int_0^\infty t f_{\hat{t}_B}(t)\,dt = \frac{1}{1 - e^{-\lambda_B C_T}} \int_0^\infty \lambda_B t e^{-\lambda_B t}\,dt = \frac{1}{\lambda_B} - \frac{1}{e^{\lambda_B C_T} - 1} C_T. \tag{22}$$

From this equation, we can summarize $E[\hat{t}_B]$ by:

$$E[\hat{t}_B] = \begin{cases} \frac{1}{\lambda_B} - \frac{1}{e^{\lambda_B C_T} - 1} C_T, & C_T > 0, \\ 0, & C_T = 0. \end{cases} \tag{23}$$

Similarly, we can have $E[\hat{t}_I]$ by:

$$E[\hat{t}_I] = \begin{cases} \frac{1}{\lambda_I} - \frac{1}{e^{\lambda_I C_T} - 1} C_T, & C_T > 0, \\ 0, & C_T = 0. \end{cases} \tag{24}$$

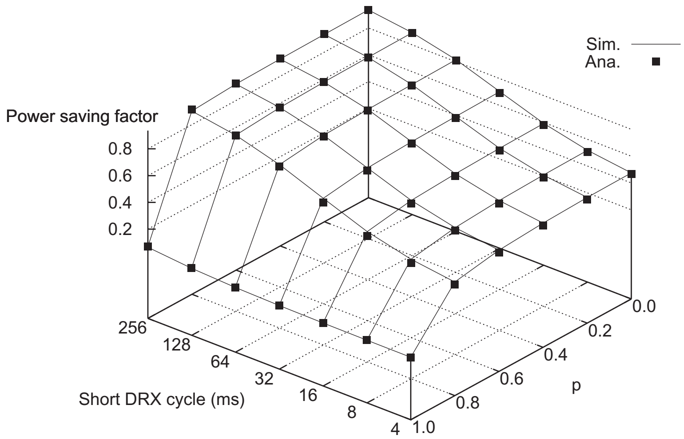

(a) Power saving factor.

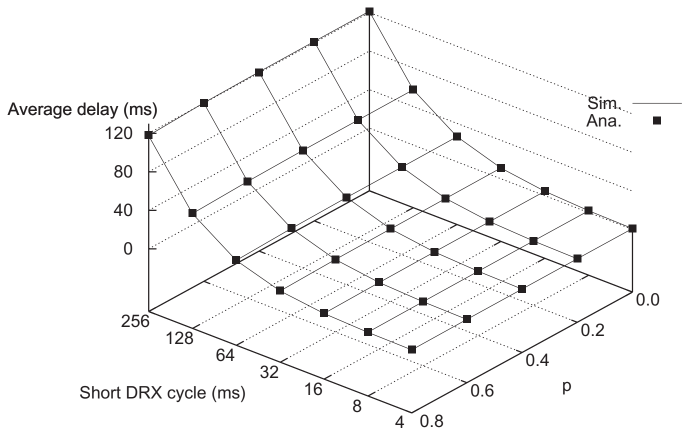

(b) Average queuing delay.

Fig. 7. Power saving factor and average queuing delay when $R = 0.1$, $C_T = 8$, $q = 0.2$, $N = 4$, $\tau = 0.1$, $\lambda_B = 1$ and $C_L = 2C_S$.

From Eqs. (23) and (24), we have:

$$E[\hat{t}] = \frac{\overline{p}_B}{\overline{p}_B + \overline{p}_I} E[\hat{t}_B] + \frac{\overline{p}_I}{\overline{p}_B + \overline{p}_I} E[\hat{t}_I]. \tag{25}$$

From Eqs. (19), (21), and (25), we can have the time durations for active state by:

$$\begin{aligned} E[T_A] &= E[\widetilde{t}_p] + \sum_{i=0}^{\infty} i\varphi_i (E[\hat{t}] + E[t_p]) + C_T \\ &= E[\widetilde{t}_p] + \frac{\varphi}{1-\varphi}(E[\hat{t}] + E[t_p]) + C_T. \end{aligned} \tag{26}$$

Finally, we complete the derivations of all equations related to power saving factor. In subsequent section, we derive average queuing delay the arriving packets may experience while passing through eNode-B.

4.3. Average queuing delay

Compared with the derivation of the power saving factor, we can derive the average queuing delay in a less complicated manner compared with the previous work [22,21,20,29,17] for the following reason: we can divide the DRX operation into two parts, i.e., immediate-transmitting and buffering-and-forwarding states, and then obtain the queuing delay in each part [24]. In this case, we can obtain the queuing delay in each part by reutilizing most equations used for the power saving factor.

In immediate-transmitting state, a newly arrived packet is immediately transmitted if eNode-B's buffer is empty. Otherwise, the arrived packets may suffer delay due to the residual time. The residual time is defined by the time required to complete packet transmissions of all packets remaining in eNode-B's buffer as well as ongoing packet transmission when a packet arrives at an arbitrary time. The delay due to the residual time is modeled by M/G/1 queuing model [24]. Accordingly, we can derive the average queuing delay in immediate-transmitting state by applying the *Pollaczek–Khinchine* (P–K) formula. Accordingly, the packet queuing delay $E[D_I]$ in immediate-transmitting state is derived by:

$$E[D_I] = \frac{\lambda E[t_X^2]}{2(1-\rho_A)}. \tag{27}$$

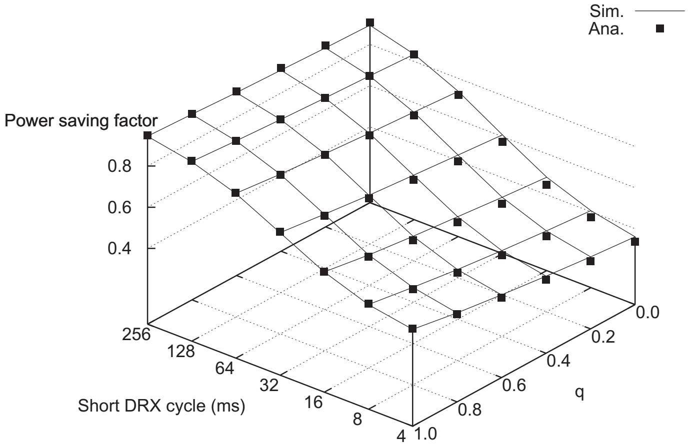

(a) Power saving factor.

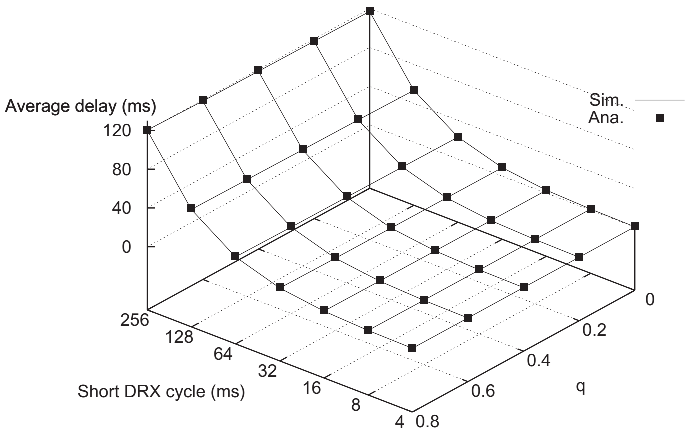

(b) Average queuing delay.

Fig. 8. Power saving factor and average queuing delay when $R = 0.1,\ C_T = 8,\ p = 0.8,\ N = 4,\ \tau = 0.1,\ \lambda_B = 1$ and $C_L = 2C_S$.

Meanwhile, in buffering-and-forwarding state, packets may experience additional delay since the packets arrived during sleeping state are not transmitted. Accordingly, there are two types of delays. One is caused by the residual time. The other is additional delay by the packet buffering operation during sleeping state. We obtain the delay due to residual time in the same way as Eq. (27), and hence, we need to derive the additional delay. For this purpose, we have two more notations, i.e., $E[K]$ and $E[W]$. $E[K]$ is average number of waiting packets in eNode-B's transmission buffer in buffering-and-forwarding state. $E[W]$ is the average waiting time of the packets arrived from the last DRX cycle. Herein, we can represent the additional delay due to the buffering operation $E[D_B]$ by:

$$E[D_B] = E[W] + E[t_X]E[K]. \tag{28}$$

According to Little's Law, $E[K] = \lambda E[D_B]$. From this equation, we can rearrange Eq. (28) by:

$$E[D_B] = E[W] + E[t_X]E[K] = E[W] + \lambda\tau E[D_B] = \frac{E[W]}{1-\rho}. \tag{29}$$

In buffering-and-forwarding state, one or more packet arrivals during any DRX cycle initiate the first activity period at the end of the DRX cycle. Then, the DRX cycle becomes the last DRX cycle prior to the first activity period. It is needed to derive the average waiting time which the arrived packets in the last DRX cycle have to wait until the beginning of the first activity period. According to the property of Poisson process, packet arrival time instants are uniformly distributed in the duration of the last DRX cycle [31]. Simply, we can obtain $E[W] = C_S/2$ or $C_L/2$ depending on which the packets arrive at, i.e., short or long DRX cycle.

In the steady state, $\lambda(E[T_A] + E[T_D])$ packets arrive during $E[T_A] + E[T_D]$ while $\lambda E[t_S]$ and $\lambda E[t_L]$ packets arrive during $E[t_S]$ and $E[t_L]$, respectively. Therefore, we can derive the probabilities P_S and P_L that packets suffer delays of $C_S/2$ and $C_L/2$, respectively by:

$$P_S = \frac{\lambda E[t_S]}{\lambda(E[T_A] + E[T_D])}, \tag{30}$$

$$P_L = \frac{\lambda E[t_L]}{\lambda(E[T_A] + E[T_D])}. \tag{31}$$

Table 2
The differences when $R = 0.1,\ N = 4,\ p = 0.8,\ q = 0.2,\ \tau = 0.1,\ \lambda_B = 1$ and $C_L = 2C_S$.

	C_S						
	4	8	16	32	64	128	256
C_T	Power saving factor differences						
0	0.04	0.04	0.05	0.03	0.01	0.00	0.01
4	0.02	0.03	0.03	0.03	0.02	0.00	0.01
8	0.01	0.01	0.01	0.01	0.01	0.00	0.01
16	0.00	0.00	0.00	0.00	0.00	0.00	0.00
32	0.00	0.00	0.00	0.00	0.00	0.00	0.00
C_T	Average queuing delay differences						
0	0.47	0.60	0.68	0.65	0.79	0.76	0.69
4	0.36	0.48	0.63	0.65	0.62	0.48	0.54
8	0.16	0.25	0.33	0.36	0.31	0.23	0.01
16	0.03	0.05	0.08	0.10	0.10	0.15	0.09
32	0.01	0.00	0.00	0.00	0.03	0.08	0.27

Table 3
The differences when $R = 0.1,\ C_T = 8,\ q = 0.2,\ N = 4,\ \tau = 0.1,\ \lambda_B = 1$ and $C_L = 2C_S$.

	C_S						
	4	8	16	32	64	128	256
p	Power saving factor differences						
0.0	0.01	0.01	0.01	0.01	0.01	0.00	0.00
0.2	0.01	0.02	0.01	0.01	0.01	0.00	0.00
0.4	0.02	0.02	0.02	0.01	0.01	0.00	0.00
0.6	0.02	0.02	0.02	0.02	0.01	0.00	0.00
0.8	0.02	0.03	0.03	0.03	0.02	0.00	0.01
1.0	0.00	0.00	0.00	0.00	0.00	0.00	0.01
p	Average queuing delay differences						
0.0	0.10	0.10	0.06	0.00	0.02	0.07	0.34
0.2	0.13	0.13	0.14	0.08	0.01	0.06	0.48
0.4	0.18	0.20	0.19	0.14	0.01	0.08	0.47
0.6	0.25	0.30	0.33	0.27	0.21	0.24	0.28
0.8	0.36	0.48	0.63	0.65	0.62	0.48	0.54

Table 4
The differences when $R = 0.1,\ C_T = 8,\ p = 0.8,\ N = 4,\ \tau = 0.1,\ \lambda_B = 1$ and $C_L = 2C_S$.

	C_S						
	4	8	16	32	64	128	256
q	Power saving factor differences						
0.0	0.02	0.03	0.04	0.03	0.02	0.00	0.01
0.2	0.02	0.03	0.03	0.03	0.02	0.00	0.01
0.4	0.02	0.02	0.03	0.02	0.01	0.00	0.01
0.6	0.01	0.02	0.02	0.01	0.01	0.00	0.01
0.8	0.01	0.01	0.01	0.01	0.00	0.00	0.00
1.0	0.00	0.00	0.00	0.00	0.00	0.00	0.01
q	Average queuing delay differences						
0.0	0.33	0.44	0.54	0.49	0.51	0.55	0.31
0.2	0.36	0.48	0.63	0.65	0.62	0.48	0.54
0.4	0.38	0.54	0.71	0.82	0.99	0.84	0.84
0.6	0.39	0.56	0.78	1.02	1.23	1.05	1.07
0.8	0.33	0.46	0.70	0.91	1.27	1.19	0.49

From Eqs. (27)–(30), we obtain average packet queuing delay by:

$$E[D] = (1 - P_S - P_L)E[D_I] + P_S\left(E[D_I] + \frac{C_S}{2(1-\rho)}\right) + P_L\left(E[D_I] + \frac{C_L}{2(1-\rho)}\right) = \frac{\lambda E[t_X^2]}{2(1-\rho_A)} + P_S\frac{C_S}{2(1-\rho)} + P_L\frac{C_L}{2(1-\rho)}. \quad (32)$$

We have derived the equations for the power saving factor and the average queuing delay, respectively. In the subsequent section, we validate our derivations by comparing with simulation results.

5. Evaluations

We validate the derived equations by comparing the analytical results with the simulation results. For this purpose, we have built a simulator running in a Linux environment. The simulator is written in 'C' language. For the simulation results in the steady state, we conduct the simulations, each of which is run for one million milliseconds of simulation time. In order to observe how DRX operational parameters influence the power saving factor and the average queuing delay, we evaluate these metrics in terms of inactivity timer C_T, the ratio R between two types of packet arrival rates, and the transition probability p. By default, we consider $p = 0.8$ and $q = 0.2$ since busy packets may arrive in more bursty manner than idle packets. In Figs. 6 and 7, the well-matched analysis and simulation results show that the equations are correctly derived.

Fig. 6 illustrates the power saving factor and the average queueing delay depending on the inactivity timer. In this figure, we can find an interesting fact. The power saving factor increases for a small value of short DRX cycle in reverse proportion to inactivity timer while the queuing delay keeps unchanged. We can explain the reason as follows: the buffered packets during the DRX cycles take the biggest part of the overall average queuing delay. However, due to small value of short DRX cycle, buffered packets are not so many during the DRX operation, and hence, the queuing delay is not so long in the first activity period. Meanwhile, packets arriving during ongoing inactivity timer may be immediately forwarded to the UE so that the queuing delays are ignorable compared with the delay in the first activity period. From this fact, we can find it out that the inactivity timer is not helpful for a small value of short DRX cycle.

Fig. 7 shows the power saving factor and the average queuing delay while state transition probability p varies from 0 to 1. Extremely, when $p = 1$, there exist only busy packet arrivals. In contrast, when $p = 0$, none of busy packets arrive. Therefore, the power saving factor has a small value when $p = 1$. Fig. 8 illustrates both the power saving factor and the average queuing delay depending on the state transition probability q. Differently from the case of the probability p, the power saving factor increases in proportion to the probability q. It is because only idle packets arrive for $q = 1$.

Tables 2–4 contain the absolute values of the differences between the analytical results and the simulation results plotted in Figs. 6–8 in turn with given parameters. The values in the tables imply that the errors are negligible.

6. Conclusion

We provide not only a novel bursty traffic model but also an easy way toward analyzing the DRX operation with the bursty traffic model. Additionally, the provided traffic model is more comprehensive than the previous work since it can be used to handle packet arrival rate changes as well as bursty packet arrivals. Therefore, we expect our work may contribute to future studies on the analysis of the power saving schemes in wireless networks with more realistic scenarios.

Acknowledgment

This work was supported by Daegu University Research Grant, 2013.

References

[1] IEEE 802.16-2009, Part 16: Air Interface for Broadband Wireless Access Systems, May 2009.
[2] IEEE 802.16m, Part 16: Air Interface for Broadband Wireless Access Systems: Advanced Air Interface, May 2011.
[3] IEEE 802.11-2012, Part 11: Wireless LAN Medium Access Control (MAC) and Physical Layer (PHY) Specifications, March 2012.
[4] Y. Xiao, Energy saving mechanism in the IEEE 802.16e wireless MAN, IEEE Commun. Lett. 9 (7) (2005) 595–597.
[5] L. Kong, G.K. Wong, D.H. Tsang, Performance study and system optimization on sleep mode operation in IEEE 802.16e, IEEE Trans. Wireless Commun. 8 (9) (2009) 4518–4528.
[6] S. Jin, X. Chen, D. Qiao, Analytical modeling of inactivity timer in IEEE 802.16m sleep mode, IEEE Commun. Lett. 16 (5) (2012) 650–653.
[7] S. Jin, X. Chen, D. Qiao, S. Choi, Adaptive sleep mode management in IEEE 802.16m wireless metropolitan area networks, Elsevier Comput. Networks 55 (16) (2011) 3774–3783.
[8] S. Jin, K. Han, S. Choi, Idle mode for deep power save in IEEE 802.11 WLANs, J. Commun. Networks (JCN) 12 (5) (2010) 480–491.
[9] Y. He, R. Yuan, X. Ma, J. Li, Analysis of the impact of background traffic on the performance of 802.11 power saving mechanism, IEEE Commun. Lett. 13 (3) (2009) 164–166.
[10] Y. He, R. Yuan, A novel scheduled power saving mechanism for 802.11 wireless LANs, IEEE Trans. Mobile Comput. 8 (2009) 1368–1383.
[11] 3GPP, Technical Specification 3G TS 36.304 Version 10.0.0, December 2010.
[12] 3GPP, Technical Specification 3G TS 36.300 Version 10.0.0, June 2010.
[13] 3GPP, Technical Specification 3G TS 36.304 Version 9.0.0, September 2009.
[14] 3GPP, Technical Specification 3G TS 36.300 Version 9.0.0, August 2009.
[15] F.-W. Li, Y.-Q. Zhang, L.-W. Li, Enhanced discontinuous reception mechanism for power saving in TD-LTE, in: Proc. ICCSIT'10, 2010.
[16] S.-R. Yang, Y.-B. Lin, Modeling UMTS discontinuous reception mechanism, IEEE Trans. Wireless Commun. 4 (1) (2005) 312–319.
[17] S.-R. Yang, Dynamic power saving mechanism for 3G UMTS system, Mobile Networks Applicat. 12 (1) (2007) 5–14.
[18] S. Yang, M. Yoo, Y. Shin, Adaptive discontinuous reception mechanism for power saving in UMTS, IEEE Commun. Lett. 11 (1) (2007) 40–42.
[19] S.-R. Yang, P. Lin, P.-T. Huang, Modeling power saving for GAN and UMTS interworking, IEEE Trans. Wireless Commun. 7 (12) (2008) 5326–5335.
[20] L. Zhou, H. Xu, H. Tian, Y. Gao, L. Du, L. Chen, Performance analysis of power saving mechanism with adjustable DRX cycles in 3GPP LTE, in: Proc. VTC'08-Fall, 2008.

[21] J.-H. Yeh, J.-C. Chen, C.-C. Lee, Comparative analysis of energy-saving techniques in 3GPP and 3GPP2 systems, IEEE Trans. Vehicular Technol. 58 (1) (2009) 432–448.
[22] C.S. Bontu, E. Illidge, DRX mechanism for power saving in LTE, IEEE Commun. Mag. 47 (6) (2009) 48–55.
[23] Y.Y. Mihov, K.M. Kassev, B.P. Tsankov, Analysis and performance evaluation of the DRX mechanism for power saving in LTE, in: Proc. IEEE IEEEI'10, 2010.
[24] S. Jin, D. Qiao, Numerical analysis of the power saving in 3GPP LTE advanced wireless networks, IEEE Trans. Vehicular Technol. 61 (4) (2012) 1779–1785.
[25] J. Huang, F. Qian, A. Gerber, Z.M. Mao, S. Sen, O. Spatscheck, A close examination of performance and power characteristics of 4G LTE networks, in: Proc. ACM MobiSys'12, 2012.
[26] M. Polignano, D. Vinella, D. Laselva, J. Wigard, T. Sorensens, Power savings and QoS impact for VoIP application with DRX/DTX feature in LTE, in: Proc. VTC Spring'11, 2011.
[27] V. Mancuso, S. Alouf, Power save analysis of cellular networks with continuous connectivity, in: Proc. IEEE WoWMoM'11, 2011.
[28] S. Alouf, V. Mancuso, N. Choungmo Fofack, Analysis of power saving and its impact on web traffic in cellular networks with continuous connectivity, Pervas. Mobile Comput. 8 (5) (2012) 646–661.
[29] S.-R. Yang, S.-Y. Yan, H.-N. Hung, Modeling UMTS power saving with bursty packet data traffic, IEEE Trans. Mobile Comput. 6 (12) (2007) 1398–1409.
[30] ETSI, Universal Mobile Telecommunications System (UMTS), Selection Procedures for the Choice of Radio Transmission Technologies of the UMTS, Technical Report UMTS 30.03 Version 3.2.0, April 1998.
[31] S.M. Ross, Stochastic Processes, John Wiley & Sons, New York, 1983.

Sunggeun Jin (M'08) received the B.S. and M.S. degrees from Kyungpook National University, Daegu, Korea, in 1996 and 1998, respectively, and the Ph.D. degree from Seoul National University, Seoul, Korea, in 2008. Since 1998, he had been with the Electronics and Telecommunications Research Institute, Daejeon, Korea. He joined Daegu University, March 2013. He has participated in standard developments, including IEEE 802.11v, IEEE 802.16j, IEEE 802.16m, and IEEE 802.11ad. He also has much experience in implementing wireless networks, including mobile Worldwide Interoperability for Microwave Access, Third-Generation Partnership Project Universal Mobile Telecommunications Systems, and Wi-Fi.

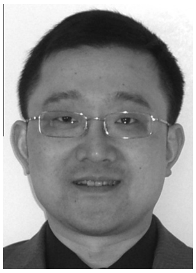

Daji Qiao received the PhD degree in electrical engineering systems from the University of Michigan, Ann Arbor, in February 2004. He is currently an associate professor in the Department of Electrical and Computer Engineering, Iowa State University, Ames, Iowa, USA. His current research interests include protocol and algorithm innovation and implementation for IEEE 802.11 wireless local area networks and wireless sensor networks, cyber security and cloud computing, and pervasive computing applications. He is a member of the IEEE and ACM.